2015 International Conference on Unmanned Aircraft Systems (ICUAS)
Denver Marriott Tech Center
Denver, Colorado, USA, June 9-12, 2015

Adaptive UKF-SLAM based on Magnetic Gradient Inversion Method for Underwater Navigation

Meng Wu[1] , Jian Yao[2]

12 School of Remote Sensing and Information Engineering, Wuhan University, P.R. China

Abstract: Consider the two characteristics: (1) Simultaneous localization and mapping (SLAM) is a popular algorithm for autonomous underwater vehicle, but visual SLAM is significantly influenced by weak illumination. (2)Geomagnetism-aided navigation and gravity-aided navigation are equally important methods in the field of vehicle navigation, but both are affected heavily by time-varying noises and terrain fluctuations. However, magnetic gradient vector can avoid the influence of time-varying noises, and is less affected by terrain fluctuations. To this end, we propose an adaptive SLAM-based magnetic gradient aided navigation with the following advantages: (1) Adaptive SLAM is an efficient way to deal with uncertainty of the measurement model. (2) Magnetic gradient inversion equation is a good alternative to be used as measurement equation in visual SLAM-denied environment. Experimental results show that our proposed method is an effective solution, combining magnetic gradient information with SLAM.

Keywords: Adaptive SLAM; magnetic gradient vector; magnetic gradient inversion equation.

I Introduction

The simultaneous localization and mapping (SLAM) algorithm was first proposed by Smith and Cheeseman in 1988 to provide localization and map building for mobile vehicles, and first used for an unmanned underwater vehicle (UUV) navigation in September 1997 in a collaborative project between the Naval U□□□ □□“ □□□ □C□□ □ (□C“ C) □□□5 □□□□□□“ □□□ Sous-□ □ □□□ □□ □A □□□ □ □□(5 “A□ A). B □□□V□□□ □□□ □□□A: A□ □□ to get a UUV starting in an unknown location and without previous knowledge of the environment, to build a map via its onboard sensors and □□ □ □ □ □□ □□□ □□ □□□ □□□□□ □□□□□□ □□ □□□□□□, A: A□ is widely used in visual navigation because vision is the richest source of information from our environment [1][3]. The visual SLAM techniques can be classified into using stereo camera [4][5] and monocular camera [6-9].

From [2], it is clear that visual SLAM has its disadvantages in mobile vehicle, which is affected greatly by illumination and camera pose. If a camera is in an environment with poor illumination, visual signals cannot be obtained exactly to be used as landmarks in visual SLAM, and a large measurement bias from a camera cannot guarantee that the unscented Kalman filter (UKF)-SLAM has a good convergence [16]. Finally, the estimated location cannot be accurate enough. In particular, in the underwater environment, visual signals from stereo cameras are easily distracted by weak illumination, which brings large measurement errors into UKF-SLAM. Compared with the visual SLAM method, geophysical navigation approach is less affected by weak illumination, and is more suitable for the autonomous underwater vehicle to acquire navigation updates by surfacing or nearly surfacing [10][11]. Therefore, SLAM based on geophysical information is an alternative in cases of visual signal drop-off. Liu et al. introduced a kind of SLAM-based geomagnetic aided inertial navigation method to improve the accuracy of navigation and localization system [12]. Wang et al. combine geomagnetic navigation algorithm together with SLAM to realize an autonomous navigation system [13].

In the field of underwater object detection based on magnetic gradient tensor, Yu Huang et al. proposed a localization method combined with magnetic gradient tensor and draft depth [17]. Hao yan-ling et al. put forward an existing solution, where the geomagnetic anomaly is inversed a magnetic dipole target and the relative position of the vehicle is determined by magnetic magnitude and gradients of targets [18].

Considering various kinds of time-varying noises and terrain fluctuations, and especially given that the variations in gravity or geomagnetism are insufficient in some areas, we add magnetic gradient information into SLAM to improve the accuracy of UKF-SLAM. In our method, the magnetic gradient values of landmarks are measured by seven magnetometers which are installed on an underwater vehicle. According to magnetic gradient values, and combining a method from [18][19], it is easy to obtain a relative position between a landmark and underwater vehicle. Then, an adaptive UKF is combined with SLAM to find a series of optimal estimations for the underwater vehicle in different discrete times. According to such estimations, the vehicle can navigate itself without any reference maps. This paper is organized as follows. In Section 2, the state and measurement models of a navigation system are introduced and analyzed. In section 3, the adaptive UKF-SLAM algorithm is presented. In Section 4, experiment and stimulation results are discussed. Conclusions and future work are summarized in Section 5.

Corresponding author: Meng Wu (wumenghust911@gmail.com)

II SYSTEM STATE AND MEASUREMENT EQUATIONS

(a) Introduction of State Equation

System state equation can be described in a kind of vehicle kinematics which is given in the below form:

$$\begin{cases} X_{t+1} = \begin{bmatrix} x_{t+1} \\ y_{t+1} \\ z_{t+1} \\ \psi_{t+1} \\ u_{t+1} \\ v_{t+1} \\ \omega_{t+1} \\ r_{t+1} \\ P_{i(t+1)} \end{bmatrix} = \hat{\Phi}(X_t, u) + n_t = \begin{bmatrix} x_t + u_t T\cos(\psi_t) - v_t T\sin(\psi_t) \\ y_t + u_t T\sin(\psi_t) + v_t T\cos(\psi_t) \\ z_t + \omega_t T \\ \psi_t + rT \\ u_t \\ v_t \\ \omega_t \\ r_t \\ P_{i(t)} \end{bmatrix} + n_t \\ X_t = [x_t, y_t, z_t, \psi_t, u_t, v_t, \omega_t, r_t, P_{\text{it}}]^T \end{cases} \tag{1}$$

where $X_t = [x_t, y_t, z_t, \psi_t, u_t, v_t, \omega_t, r_t, P_{\text{it}}]^T$ includes the position and heading of underwater vehicle and the coordinates of a landmark (p_{it}). $[u_t, v_t, \omega_t, r_t]$ are the line velocity and angle velocity of the underwater vehicle and T is the sample time. n_t is system noise with covariance matrix given by R.

$$\begin{cases} E\left[(n_t - q_t)(n_j - q_j)^T\right] = \delta_{ij} R_t \\ E[n_t] = q_t \end{cases} \tag{2}$$

In the underwater environment, the method in [14] is a good solution to calculate relative distance and orientation between a landmark and underwater vehicle.

The coordinates of a landmark is as follows:

$$\text{p}_{\text{it}} = \begin{bmatrix} \text{x}_{\text{it}} \\ \text{y}_{\text{it}} \end{bmatrix} \tag{3}$$

Where x_{it} and y_{it} stand for the i^{th} □□□□ □□□ □□ □□□□ □□□□ ation at the time t in the direction of x and y, respectively. In general, the position of a static landmark varies minimally in the different time t

$$p_{i(t+1)} = p_{it} = p_i, i = 1, 2, \cdots\cdots, N \tag{4}$$

(b) Introduction of Measurement Equation

Ferromagnetic objects can cause geomagnetic anomaly and they are usually treated as underwater magnetic targets which are only several hundreds nano-Tesla [17]. When an underwater magnetic target is far from an underwater vehicle, the target can be treated as a magnetic dipole and described as follows [17-19]:

$$\begin{cases} B = \dfrac{\mu}{4\pi}\left[\dfrac{3(m \cdot r)r}{r^5} - \dfrac{m}{r^3}\right] \\ r = {}_X e_x + {}_Y e_Y + {}_Z e_Z \end{cases} \tag{5}$$

Where μ denotes susceptibility of the medium and r denotes position vector of measuring point P (X, Y, and Z). m denotes target magnetic moment

vector, whose components are m_x, m_y, and m_z, respectively [17][19]. Based on the equations deduced from [17][19], magnetic gradient components, the relative localization between an underwater magnetic target and underwater vehicle can be expressed as Eqs. (6)(7)(8):

$$\begin{cases} \dfrac{\partial B_x}{\partial X} = a = \dfrac{3\mu}{4\pi}\dfrac{x\left(3r^2-5x^2\right)m_x + y\left(3r^2-5x^2\right)m_y + z\left(3r^2-5x^2\right)m_z}{r^7} \\ \dfrac{\partial B_y}{\partial Y} = b = \dfrac{3\mu}{4\pi}\dfrac{x\left(3r^2-5y^2\right)m_x + y\left(3r^2-5y^2\right)m_y + z\left(3r^2-5y^2\right)m_z}{r^7} \\ c = -(a+b) \\ \dfrac{\partial B_y}{\partial X} = d = \dfrac{3\mu}{4\pi}\dfrac{y\left(3r^2-5x^2\right)m_x + x\left(3r^2-5x^2\right)m_y - 5xyzm_z}{r^7} \\ \dfrac{\partial B_z}{\partial Y} = e = \dfrac{3\mu}{4\pi}\dfrac{z\left(r^2-5y^2\right)m_y + y\left(r^2-5z^2\right)m_z - 5xyzm_x}{r^7} \\ \dfrac{\partial B_z}{\partial X} = f = \dfrac{3\mu}{4\pi}\dfrac{z\left(r^2-5x^2\right)m_x + x\left(r^2-5z^2\right)m_z - 5xyzm_y}{r^7} \end{cases} \tag{6}$$

$$\begin{cases} A_6k^6 + A_5k^5 + A_4k^4 + A_3k^3 + A_2k^2 + A_1k^1 + A_0 = 0 \\ A_6 = d^2(a+2b) - e^2(a-b) + 2def \\ A_5 = -2d\left[(a-b)(a+2b) + \left(d^2+e^2+f^2\right)\right] \\ A_4 = (a-b)^2(a+2b) + d^2(4a-7b) + \left(f^2-2e^2\right)(a-b) + 6edf \\ A_3 = -4d\left[(a-b)^2 + \left(d^2+e^2+f^2\right)\right] \\ A_2 = (a-b)^2(a+2b) + d^2(4b-7a)\left(2f^2-e^2\right)(a-b) + 6edf \\ A_1 = 2d\left[(a-b)(a+2b) - \left(d^2+e^2+f^2\right)\right] \\ A_0 = d^2(a+2b) + f^2(a-b) + 2edf \end{cases} \tag{7}$$

$$\begin{cases} q = \dfrac{\left[d\left(k^2-1\right)-(a-b)k\right]}{(ek-f)\left(k^2+1\right)} \\ \Delta z = \dfrac{\pm 3}{\sqrt{\left[(ak+d)q+f\right]^2+\left[(dk+b)q+e\right]^2+\left[(fk+e)q+c\right]^2}} \\ \Delta x = kq\Delta z \\ \Delta y = q\Delta z \end{cases} \tag{8}$$

To get the values A in equation (7), it is necessary to measure magnetic gradients (a, b, d, e, f), according to the method in [18][19], seven single-axis magnetometer configuration is as the simplest scheme of measuring magnetic gradient tensor. After obtaining parameters A, the six-order Eq. (7) can be calculated to get the value of k, then, k is substituted into Eq. (8) to calculate q. Finally, the relative position (Δz, Δy, Δx) of an underwater magnetic landmark which is away from underwater vehicle can be calculated. The below equation is served as the general measurement equation.

$$Z_t = \mathrm{h}\left(x_{t+1}\right) + \delta_k \tag{9}$$

δ_k is an additive, zero-mean Gaussian noise and observation Z_t is a function h of the current state corrupted by additive Gaussian noise δ_k with covariance Q_k.

$$\mathrm{h}\left(x_{t+1}\right) = \begin{bmatrix} \Delta z = \dfrac{\pm 3}{\sqrt{\left[(ak+d)q+f\right]^2+\left[(dk+b)q+e\right]^2+\left[(fk+e)q+c\right]^2}} \\ \Delta x = kq\Delta z \\ \Delta y = q\Delta z \\ R(\Delta x, \Delta y, \Delta z) = \sqrt{(\Delta x)^2+(\Delta y)^2+(\Delta z)^2} \end{bmatrix} \tag{10}$$

III. INTRODUCTION OF AN ADAPTIVE UKF BASED SLAM

A block diagram of adaptive UKF-SLAM based on magnetic gradient algorithm is shown in Fig. 1. According to the method mentioned in [19], the relative positions between landmarks and underwater vehicle can be calculated by magnetic gradient inversion method. The gyroscope and accelerometer provide the state information of underwater vehicle. Based on the state and measurement equations, adaptive UKF-SLAM is used to update the state of this underwater vehicle navigation system. Then the underwater vehicle adopts the positions of landmarks and state of its movement along a definite trajectory to locate itself and build a real environmental map simultaneously.

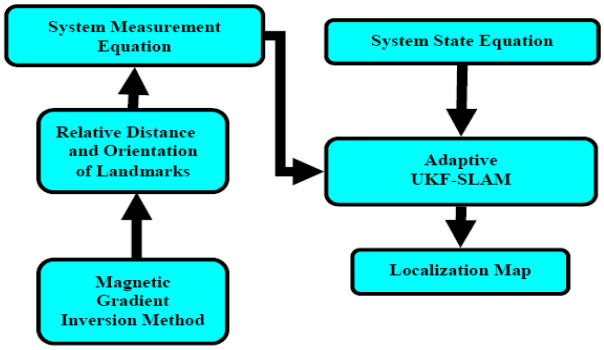

Fig. 1. The block diagram of Magnetic gradient navigation system based on adaptive UKF- SLAM

(a) Introduction of an Adaptive UKF

A wealth of literature exists on the UKF and SLAM algorithms. Here, we simply present the modified adaptive UKF equation as follows for the sake of brevity:

Step (1): Initialization

$$\begin{cases} \hat{w}_0 = E[w_0] \\ P_0 = E[(w_0 - \hat{w}_0)(w_0 - \hat{w}_0)^T] \end{cases} \tag{11}$$

Step (2): Calculation of sigma points with corresponding weights

$$\begin{cases} (\chi_t^a)_0 = \hat{x}_t^a \\ (\chi_t^a)_i = \hat{x}_t^a + (\sqrt{(L+\lambda)P_t^a})_i \qquad i = 1,\ldots,L \\ (\chi_t^a)_i = \hat{x}_t^a - (\sqrt{(L+\lambda)P_t^a})_{i-L} \qquad i = L+1,\ldots,2L \\ W_0^{(m)} = \lambda/(L+\lambda) \\ W_0^{(c)} = \lambda/(L+\lambda) + (1-\alpha^2+\beta) \\ W_i^{(m)} = W_i^{(c)} = 1/\{2(L+\lambda)\} \qquad i = 1,\ldots,2L \end{cases} \tag{12}$$

Step (3): Time update

$$\begin{cases} (\chi_{t+1|t}^a)_i = \Phi[(\chi_t^x)_i, (\chi_t^w)_i] \\ \bar{x}_{t+1|t}^a = \sum_{i=0}^{2L} W_i^{(m)} (\chi_{t+1|t}^a)_i \\ P_{t+1|t}^a = \sum_{i=0}^{2L} W_i^{(c)} [(\chi_{t+1|t}^a)_i - \bar{x}_{t+1|t}^a][(\chi_{t+1|t}^a)_i - \bar{x}_{t+1|t}^a]^T \\ (y_{t+1|t})_i = H[(\chi_{t+1|t}^x)_i] \\ \bar{y}_{t+1|t} = \sum_{i=0}^{2L} W_i^{(m)} (y_{t+1|t})_i \end{cases} \tag{13}$$

Step (4): Measurement update

$$
\begin{cases}
P^{a}_{z_{t+1|t}z_{t+1|t}} = \sum_{i=0}^{2L} W_i^{(c)}[(z_t)_i - \hat{z}_{t+1|t}][(z_t)_i - \hat{z}_{t+1|t}]^T \\
P^{a}_{x_{t+1|t}z_{t+1|t}} = \sum_{i=0}^{2L} W_i^{(c)}[(\chi^{x}_{t+1|t})_i - \hat{x}^{a}_{t+1|t}][(z_{t+1|t})_i - \hat{z}_{t+1|t}]^T \\
v_t = (z_t)_i - \hat{z}_{(t+1|t)(i)} \\
\Gamma_t = tr\left(P^{a}_{z_{t+1|t}z_{t+1|t}}\right) \\
\sigma_t = \begin{cases} v_t v_t^T \,(t=1) \\ \dfrac{\rho\sigma_t + v_t v_t^T}{(1+\rho)\Gamma_t}\,(t>1) \\ 0 \le \rho \le 1 \end{cases} \\
\kappa_{t+1} = \sigma_t P^{a}_{x_{t+1|t}z_{t+1|t}} (P^{a}_{z_{t+1|t}z_{t+1|t}})^{-1} \\
\hat{x}^{a}_{t+1} = \hat{x}^{a}_{t+1|t} + \kappa_{t+1}(z_{t+1} - \hat{z}_{t+1|t}) \\
P^{a}_{t+1} = P^{a}_{t+1|t} - \kappa_{t+1} P^{a}_{z_{t+1|t}z_{t+1|t}} \kappa_{t+1}^T
\end{cases}
\tag{14}
$$

In Eq. (14), the parameter ρ (forgotten parameter) and σ_t are adopted to improve the robustness of UKF and keep the measurement covariance matrix of UKF to be definitely positive. In particular, because a conventional UKF does not have the adaptive ability to respond to changes in the noise statistics, which lead to large estimation errors and cause divergence in the case of time-varying noise statistics, however, ρ and σ_t can correct measurement error covariance, adjust the filter gain matrix κ_{t+1}, and suppress filter divergence. It enhances the fast-tracking capability of the filter. Such parameters are good for the UKF to be converging in various measurement noises and outliers.

(b) State Augmentation

In this paper, the state vector consists of the □□□□ □□□ □□ □□□□ pose, orientation, and the positions of M landmarks[1][2][5]

$$
\begin{cases}
x = [x_{R_k}^T \quad P_L^T] = [x_{R_k}^T \quad P_{L_1}^T \quad \cdots \quad \cdots \quad P_{L_M}^T]^T \\
P_{k/k} = \begin{bmatrix} P_{RR\,k|k} & P_{RL\,k|k} \\ P_{RL\,k|k}^T & P_{LL\,k|k} \end{bmatrix} \\
x_{Rk}^T = [x_t, y_t, z_t, \psi_t, u_t, v_t, \omega_t, r_t] \\
P_L^T = P_{\mathrm{it}} = \begin{bmatrix} \mathrm{x_{it}} \\ \mathrm{y_{it}} \end{bmatrix}
\end{cases}
\tag{15}
$$

Where $P_{RR\,k|k}$ denotes error covariance matrix only associated with the underwat□ □□ □□□□□ □□ □ □ □□; $P_{RL\,k|k}$ is the cross-covariance matrix between underwater vehicle and landmark states; and $P_{LL\,k|k}$ is the map covariance matrix only associated with underwater landmark state estimates. As the underwater vehicle is moving, new landmarks are observed and must be added to the stored maps, as a result, the state vector and covariance matrix are extended with the new observation z and its covariance Q. [1][5][6]:

$$
\begin{cases}
X_{aug} = \begin{bmatrix} x \\ z \end{bmatrix} \\
P_{aug} = \begin{bmatrix} P_{RR\,k|k} & P_{RL\,k|k} & 0 \\ P_{RL\,k|k}^T & P_{LL\,k|k} & 0 \\ 0 & 0 & Q \end{bmatrix}
\end{cases}
\tag{16}
$$

(c) Data Association

Because within the adaptive UKF framework, both the landmark location estimates and landmark observations are assumed to have Gaussian uncertainty, any given observation might correspond to any landmark. However, to reject unlikely associations, only landmarks within a reasonable neighbourhood of an observation should be considered. Association validation is usually performed in observation space, and a validation gate defines the maximum permissible discrepancy between a measurement Z_t and a predicted observation $\hat{z}_{t+1|t}$.

In the paper, the normalised innovation squared (NIS) is used as data association method. Given an observation innovation $v_t = (z_{t+1|t})_i - \hat{z}_{t+1|t}$ with covariance matrix S_t, the NIS is defined as

$$
M_t = v_t^T S_t^{-1} v_t \tag{17}
$$

A gate named γ is applied as a maximum NIS threshold $M_t \le \gamma$. In the paper, the gate $\gamma = 6.0$ will accept 95% of correct association, as 95% of the χ^2 distribution mass lies between 0 and 6.0.

IV. SIMULATION RESULTS

In the simulation, we assumed that the state covariance $\mathrm{R_k}$ and measurement covariance Q_{k} are Gaussian White noises. In practice, magnetometers are high-accuracy measurement sensors, and measurement covariance Q_{k} is not necessary to be set as a big value. The system state of underwater vehicle is assumed to be stable and the system covariance $\mathrm{R_k}$ is also a small value. Parameters are shown in Table.1.

Table.1. Parameters of the Adaptive-UKF-SLAM based on Magnetic Gradient Information

Initial Parameters	Values
x_0 (m)	100~150
y_0 (m)	300
z_0 (°)	0
ψ_0 (°)	0.5
u_0 (m/s)	25
v_0 (m/s)	30
r_0 (°/s)	15
ω_0 (°/s)	35
$\mathrm{R_k}$ (E^2)	10^{-4}
Q_{k} (E^2)	10^{-2}
m_x	10^6 $A \bullet m^2$
m_y	2X10^5 $A \bullet m^2$
m_z	10^5 $A \bullet m^2$

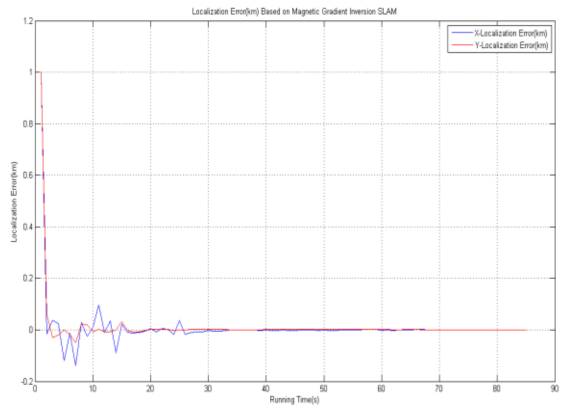

Fig.2. Localization errors of adaptive UKF-SLAM based on magnetic gradient inversion method

From Fig.2, the red and blue curves denote X and Y localization errors, respectively. It is clearly seen that the localization errors converge to zero soon. The fluctuations of the curves show that magnetic gradient inversion method is affected by the accuracy of magnetometers. If magnetometers are not accurate enough to measure magnetic gradient tensors, the magnetic gradient inversion method cannot calculate the accurate relative position between a landmark and the underwater vehicle. As a result, measurement outliers and errors affect the localization performance of SLAM.

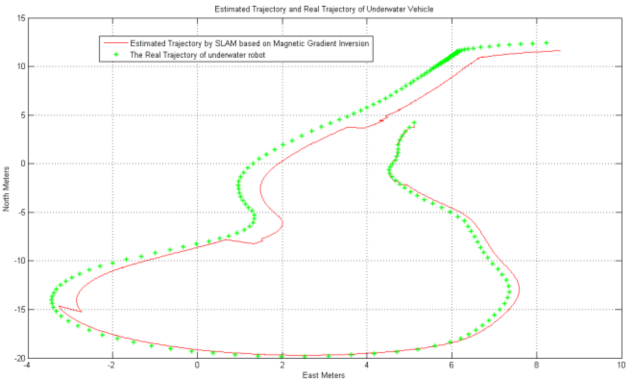

Fig. 3. The estimated and real trajectory of an underwater vehicle

From Fig. 3, the red curve denotes a real trajectory of underwater vehicle. The green curve is the estimated trajectory of underwater vehicle using adaptive SLAM based on magnetic gradient inversion method. It is clearly seen that biases between the estimated trajectory and real trajectory of underwater vehicle are in a controllable level and such biases arise from measurement errors of magnetometers.

I. CONCLUSIONS

The paper proposes a kind of SLAM based on adaptive UKF method and combines magnetic gradient inversion method to locate the underwater vehicle itself. Based on the experimental results, it proves that SLAM based on adaptive UKF with magnetic gradient inversion method is feasible under harsh and real-time underwater condition. In particular, magnetic gradient vectors are less affected by time-varying disturbances, and adaptive UKF is a better way to robustness towards various measurement outliers and noises.

In future work, one important issue is how to improve the robustness of SLAM based on adaptive UKF against strong electromagnetic disturbances; the other is how to improve the measuring accuracy of magnetometers and to pay more attention to sensor calibration.

REFERENCES

[1] H. Durrant-"e and B. B e, A and apping (A A): pa ," Robo c an Au o a ion S , vo 13, 2, pp. 99-108, 2006.

[2] T. Bailey and H. Durrant-"e ," A S and apping (A A): ," botics and Automation Magazine, vol. 13, no. 3, pp. 108-117, 2006.

[3] Wang Fei, Cui Jin-Qiang, Chen Ben- , : Bong H , A Comprehensive UAV Indoor Navigation System Based on Vision Optical an : ae 4 A A." ACBA ACB AB CA A CA, D .39, No.11, pp. 1890-1900, November, 2013.

[4] R. Sim, P. Elinas, M. Griffin, and J.J. : , D -based SLAM using the Rao-B , CA" on R a o ing Uncertainty in Vehicleics (RUR), 2005.

[5] A.J. Davision, I. Reid, N. , O. A , A: A : -time ing A: A ", " B on Pa e n A e Intelligence, vol. 29, No.6, pp: 1052-1067, 2007.

[6] A. D , -time simultaneous localization and mapping with a ing c e a" roc. International Conference on Computer Vision, Nice, October 2003.

[7] T. B e, C S e , Conf. on Vehicleics and Automation, ICRA, Taipei, Taiwan, pp.1966-1971.2005.

[8] Sunhyo Kim and Se- , Slam in indoor environments using omni- a d S ", and Vehicleics Systems, vol.51, no.1, pp: 31-43, January 2008.

[9] Young-Ho Choi and Se- , 5 -based visual slam in complex environme , Jou a of nd D Ae , vo 50, 3, pp: 241-255, November 2007.

[10] Z ng H., " , H., " , : ., C , H., " , 5 . A Re c on Gravity-5 Co ined A C de wa e Naviga io ," e Institute of Navigation, vol. 66, No. 1, pp: 83-98, 2013.

[11] " , : ., B , 4 ., , H. B , ," , C V D B on 5 e 5 , " 5 nd Re o e A : ters, Vol. 7, No. 2, pp: 362-365, 2010

[12] Liu Ming, Wang Hai-Jun, Jiang Yan-A , Ae ode ng of SLAM- 5 A Navig i ," A Manufacturing Technology, vol. 47, No. 6, pp: 13-16, 2011.

[13] Shi-cheng Wang, da-wei Sun, Jin-Sheng, Zhang, Li-hua, Chen, Re c on 5 o agnei Navig n an : S B on A: A ," Fire Control & Command Control, vol. 35, no.12, pp: 35-37, 2010.

[14] Lin Wu, Xin Tian and Jie Ma et al, " Jnderwater Object Detection Based on Gravity Gradient," IEEE Geoscience and Remote Sensing Letters, vol. 7, no.20, pp:362-365, 2010.

[15] S. Julier, J. Uhlmann, and H. F. Durrant-"e , A e od e of a d nd e a o ," IEEE Transactions on Automatic Control, vol. 45, no.3, pp: 477-482, 2000.

[16] S.J. Julier and J.K. C l nn, C an , " P o edin of e " , 92, 3, : 401-422, 2004.

[17] Yu Huang, Li-Hua Wu, and Feng Sun C de wa e C n nuou Localization Based on Magnetic Dipole Target Using Magnetic Gradient Tensor and Draft Depth, *"IEEE Geosci. Remote Sens.Lett.vol.11,no.1, pp.178-180, Jan .2014.*

[18] Hao yan-ling, Zhao ya-feng, Hu jun-feng e ana e i on e application of geomagnetic field matching in underwater vehicle navigation, *Progress in Geophysics. Vol.18, pp.64-67, Feb. 2008.*

[19] Yu Huang, Sun Feng, Hao Yan- A agne o e e configuration scheme to measure magnetic field gradient tensor, *Proceedings of* the *2010 IEEE International Conference on Mechatronics and Automation. Vol.5, pp. 1426-1430, August. 2010.*